On the Freezing Time of Supercooled Drops in Developing Convective Clouds

Jing Yang[1], Zhien Wang[1], and Andrew Heymsfield[2]

[1] {Department of Atmospheric Science, University of Wyoming, Laramie, WY}

[2] {National Center for Atmospheric Research, Boulder, CO}

Correspondence to: Zhien Wang (zwang@uwyo.edu)

Submitted to

Atmospheric Chemistry and Physics Discussion

Abstract

Ice generation and evolution in convective clouds are still poorly understood and challenging to model. Aircraft measurements during the Ice in Clouds-Tropical (ICE-T) project suggest that the observed ice particles in intense convective clouds are primarily small at relatively warm temperature (between -7 °C and -10 °C), and large frozen drops are detected at a colder temperature than -10 °C. However, the ice particle size distributions (PSDs) between -7 °C and -10°C modelled using a parcel model containing a spectral bin microphysics scheme are much

Deleted: In this study, the particle size distributions (PSDs) measured in fresh developing maritime convective clouds sampled during the Ice in Clouds-Tropical (ICE-T) project are shown and compared with the PSDs modeled using a parcel model containing a spectral bin microphysics scheme.

Deleted: The observations aircraft

Deleted: ed

Deleted: "first ice"

Deleted: is

Deleted: with

Deleted: e

Deleted: ezing

Deleted: were

Deleted: On the other hand

Deleted:

Deleted: ,

Deleted: but

Deleted:

Deleted: ,

Deleted: ,

Deleted: PS

broader than the observations. To interpret the difference in the temperature-dependent ice PSD evolution between the model simulations and the observations, the freezing times and temperatures of supercooled drops are modeled and interpreted. The results indicate that the freezing time (from the initial nucleation to fully frozen) must be considered; it is not instantaneous, and is longer for large drops than for small drops. In strong updrafts, such as that sampled by the Learjet during ICE-T, large freezing drops can be carried upwards to a lower temperature than their nucleation temperature before they are fully frozen. This offers a feasible explanation for the temperature-dependent ice particle size evolution in strong updrafts observed during ICE-T. In models, drop freezing is normally assumed to be instantaneous, which is not realistic; the models yields broader ice PSDs between -7 °C and -10 °C than is observed. The results highlight the importance to consider the freezing time of supercooled drops in interpreting the observed and modelled ice PSDs in fresh developing convective clouds and in modelling ice generation in cloud resolving models. To better understand the mechanisms of drop freezing and ice initiation in convective clouds, more laboratory experiments and in situ measurements are needed.

1. Introduction

Ice initiation in convective clouds is still not well understood (Cantrell and Heymsfield, 2005; Lawson et al., 2015; Yang et al., 2016), and it remains one of the main sources of uncertainties in numerical models (Khain et al., 2015). Observations suggest that ice initiation in convective clouds is strongly related to the freezing of supercooled drops and the size of the freezing drops (Rangno and Hobbs, 2005; Lawson et al., 2015; Yang et al., 2016; Field et al., 2017). Supercooled drops do not fully freeze instantaneously, and drops at the early stage of freezing usually have little if any deformation (Johnson and Hallett, 1968; Murray and List, 1972;

Deleted: at warm temperature
Deleted: in convective clouds is small
Deleted: size
Deleted: s
Deleted: ed ice PSDs
Deleted: analyzed
Deleted: freezing
Deleted: but
Deleted: it is
Deleted: Due to instrumental limitations, freezing drops cannot be identified until they exhibit obvious shape deformation. If
Deleted: the
Deleted:
Deleted: is strong enough
Deleted: obvious shape deformation occurs
Deleted: observed
Deleted: size
Deleted: observed
Deleted: the
Deleted: although there are still large uncertainties in ice generation mechanisms
Deleted: thus,
Deleted: a
Deleted: "first ice"
Deleted: is
Deleted: study allows us to
Deleted: modeled and the
Deleted: from the perspective of the freezing time of supercooled drops and notes the deficiency of instantaneous drop freezing in models
Deleted: in the future
Formatted: Font:Not Bold
Deleted: s
Deleted: no or slight

Hindmarsh et al., 2003). The freezing rate of supercooled drops depends on the rate of heat transfer between the drop and ambient air (Pruppacher and Klett, 2010). Typically, the freezing process comprises four stages (Hindmarch et al., 2003): 1) the supercooling stage, during which a drop is supercooled to its nucleation temperature; 2) the recalescence stage, during which rapid kinetic ice nucleation occurs, which results in a rapid rise in temperature that is terminated when the drop temperature reaches 0 °C; 3) the freezing stage, during which the liquid part of a drop continuously freezes and the drop temperature remains at 0 °C; and 4) the cooling stage, during which the frozen drop cools to the ambient temperature.

A number of laboratory experiments have been performed to study the freezing of supercooled drops. For example, Johnson and Hallett (1968) showed that the freezing time of supercooled drops decreases with decreasing ambient temperature. They also showed that the freezing rate of supercooled drops is related to the composition of the air and that the freezing time of a millimeter-sized drop in helium and hydrogen is only one-fifth of that in air. Hindmarsh et al. (2003) showed that the freezing time increases with increasing drop size. In addition, Hindmarsh et al. (2003) used experimental results to discuss the accuracy of three drop freezing models: the uniform temperature model, the inward freezing model and the outward freezing model. All three of these models have fairly good accuracy in modeling drop temperatures and freezing times, and there are only minor differences between them.

In most numerical weather prediction models (NWPMs) and global climate models (GCMs), the freezing of supercooled drops is assumed to be instantaneous, because it is difficult to track the freezing stage of every particle in models and because there are no good observations with which to evaluate the modeled ice microphysics in detail. Phillips et al. (2015) implemented time-dependent freezing for raindrops in a cloud model using spectral bin microphysics (SBM). Their

Deleted: during airborne measurements, freezing drops cannot be observed until they have experienced obvious deformation

Deleted: 1997

Deleted: drop

Deleted: In typical air conditions, it takes approximately 400 s for a stationary millimeter-sized drop to completely freeze at -5 °C under a pressure of 1 atm; this freezing time is reduced to approximately 200 s at -10 °C.

sensitivity tests showed that time-dependent drop freezing delays the formation of hail in convective clouds; however, their model was unable to track the freezing stage of every particle. Using a simplified cloud parcel model and an electromagnetic scattering model, Kumjian et al. (2012) showed that the modeled radar polarimetric variables for convective clouds are more consistent with observations if time-dependent drop freezing is considered. However, drop freezing in fresh developing convective clouds, such as the freezing time and the temperature of supercooled drops, has rarely been discussed.

Aircraft in situ measurements are vital for improving our current understanding of ice generation in convective clouds and to evaluate model simulations. Traditional in situ measurements can rarely identify ice that is smaller than 100 μm in diameter. The 3-View Cloud Particle Imager (3V-CPI) is a good tool with which to record images of small particles, and it can be used to identify the shapes of the small ice (Lawson et al., 2015). During the Ice in Clouds-Topical (ICE-T) project, the 3V-CPI that was operated on the SPEC Learjet yielded high-resolution particle images and particle size distributions (PSDs). The 3V-CPI measurements suggest that the observed ice at relatively warm temperature (about -8 °C) in fresh developing convective clouds are primarily small (Lawson et al., 2015); however, the results of some other studies have suggested that larger supercooled drops may freeze before smaller drops (Bigg, 1953; Heymsfield, 2013). This raises the question: are models able to capture the characteristics of the ice PSDs observed in developing convective clouds? Understanding the freezing time of supercooled drops is helpful for interpreting the difference between the observed and the modeled ice PSDs in developing convective clouds. In addition, the aircraft observations are useful for evaluating the impact of instantaneous drop freezing on the modeled PSDs.

Deleted: in fresh developing convective clouds

Deleted: Thus, to better understand ice initiation in convective clouds and to evaluate the modeled microphysics, more observations are needed.

Deleted: necessary to improve

Deleted: initiation

Deleted: 200

Deleted: image

Deleted: "first ice"

Deleted: all

Deleted: ice

Deleted: why is the observed observed ice at relatively warm temperature "first ice" in convective updrafts small?

Deleted: Is

Deleted: A

Deleted: is

Deleted: to evaluate

This study aims to better understand the impact of the freezing time and temperature of large supercooled drops on ice PSDs evolution in developing convective clouds. Observed PSDs in developing convective clouds during the ICE-T project are used to evaluate the PSDs modelled by a parcel model, and the deficiency of instantaneous drop freezing in the model simulations are discussed based on the aircraft observation and quantitative calculations of the freezing time and temperature of supercooled drops. This paper is organized as follows: Section 2 introduces the dataset and the analytical method; Section 3 discusses the results; and a summary is given in Section 4.

2. Dataset and Analysis Method

2.1 Calculation of the freezing time of supercooled drops

The calculation of the freezing time and temperature of supercooled drops is governed by a series of heat transfer and phase change equations. These detailed equations have been described in previous studies (e.g., Dye and Hobbs et al., 1968; Heymsfield, 1982; Hindmarsh et al., 2003). The drop temperature increase is balanced by convective heat transfer (i.e., ventilation), radiation and latent heat terms. In this calculation, a supercooled drop is assumed to be carried upward by an updraft, which ascends adiabatically. The terminal velocity of the drop follows that defined by Foote and Du Toit (1969). Diffusional growth is included but coalescence is neglected. Coalescence is the key process by which large supercooled drops develop in convective clouds. However, it is not necessary to include the coalescence process during the freezing of the drop in the calculation of the freezing time of a single supercooled drop, because the freezing time is the shortest assuming that drop size doesn't increase due to coalescence after freezing begins. The drop size increase due to coalescence process results in a longer freezing time. In this study, we

Deleted: determining the size of "first ice" is important for understanding secondary ice generation process(es).

Deleted: analyze the o

Deleted: using the data collected

Deleted: . The observation is

Deleted: is

Deleted: , as well as to interpret these observations through the perspective of

Deleted: change

Deleted: In this calculation, d

Deleted: to generate

Deleted: ,

Deleted: but

prefer to examine the shortest freezing time of supercooled drop for a given size. The initial drop temperature is the same as the ambient air temperature. The temperature inside the drop is assumed to be uniform; this is a reasonable assumption because water and ice have a larger thermal conductivity than air and because of the internal mixing of liquid within the drop (Yao and Schrock, 1976). Hindmarsh et al. (2003) showed that including temperature variations inside the drop has a minor impact on the results. The freezing time is defined as the time period from the start to the end of the drop freezing.

2.2 Aircraft measurements during ICE-T

The ICE-T project was conducted in July 2011 over the Caribbean Sea, near the U.S. Virgin Islands; its goal was to study ice generation in tropical maritime convective clouds. Both the National Center for Atmospheric Research (NCAR) C-130 aircraft and the SPEC Incorporated Learjet were deployed during ICE-T.

The SPEC Learjet was equipped with the state-of-art instruments that were used to study the microphysics in convective clouds during ICE-T. The primary objective of the Learjet was to make rapid, repeated penetrations in the updrafts of growing turrets. The instruments included a fast forward-scattering spectrometer probe (FFSSP); a CPI; a two-dimensional stereo (2D-S) probe; a high-volume precipitation spectrometer (HVPS-3), and a Rosemount temperature probe. The measurements obtained using the FFSSP, CPI, 2D-S, and HVPS were combined to generate the PSDs. CPI images were used to identify liquid drops and ice particles that were smaller than 500 μm in diameter, and these percentages of drops and ice particles were applied to the 2D-S PSDs. The 2D-S and HVPS images were used to identify drops and ice particles that were larger than 500 μm in diameter. More information about the processing of the Learjet data can be found

Deleted: various

Deleted: goal of the Learjet was to make repeated penetrations in fresh developing convective updrafts near the cloud top

Deleted: se

in Lawson et al. (2015).

The NCAR C-130 was not used to repeatedly penetrate fresh developing convective clouds during ICE-T; instead, it penetrated convective clouds at different stages of their development. Most of these penetrations occurred far below the cloud top, although some were near the cloud top (Heymsfield et al., 2014; Yang et al., 2016). The C-130 instruments included a Forward Scattering Spectrometer Probe (FSSP), a two-dimensional cloud (2D-C) probe, a two-dimensional precipitation (2D-P) probe, and a Rosemount temperature probe. The Wyoming Cloud Radar (WCR; Wang et al. 2012) was operated on the C-130 to obtain 2D reflectivity structures, and the Wyoming Cloud Lidar (WCL; Wang et al. 2009) was used to identify liquid-dominated and ice-dominated clouds.

2.3 Parcel model simulation

In this study, we compare the PSDs modeled using a parcel model containing SBM to those observed by the aircraft. The SBM was developed by Hebrew University (Khain et al., 2000) and has been implemented in the Weather Forecast and Research model (WRF; Lynn et al., 2005). Time-dependent drop freezing is not included in this scheme. The purpose of this simulation is not to evaluate the modeled ice concentration using observations, but instead to identify the extent of the deficiency of instantaneous drop freezing in SBM. The modeled parcel has a depth of 500 m. The observed drop size distribution at -6 °C is used as an input. The observed mean vertical velocity in the updrafts sampled by the Learjet is used in the simulation. The hydrometeor types include cloud drop/rain, ice/snow, and graupel; the PSD of each hydrometeor type has 33 mass bins. The ice nucleation mechanisms include immersion freezing using the Bigg parameterization (1953), deposition/condensation nucleation (Meyer et al., 1992), contact

Deleted: used here

Deleted: an FFSSP

Deleted: results

Deleted: reveal

Deleted: and its inability to capture the observed rapid ice generation

Deleted: The vertical air velocity is 10 m/s, which is a typical mean updraft strength in the convective clouds sampled during ICE-T

Deleted: , which is temperature-dependent,

Deleted: 's

nucleation (Meyer et al., 1992), and the Hallett-Mossop process (Hallett and Mossop, 1974). Other ice microphysics processes include riming, coalescence and diffusional growth. During every time step, 1% of the aerosols in the ambient air are assumed to become entrained into the cloud parcel. The ambient aerosol size distribution is observed using a high-flow dual-channel differential mobility analyzer (HDDMA; DeMott et al., 2016) and a Passive Cavity Aerosol Spectrometer Probe (PCASP; Baumgardner et al., 2011) operated on the C-130.

3. Results and Discussion

3.1 Comparison of observed and modeled particle size distributions

Fig. 1 shows the PSDs measured by the Learjet and those modeled using a parcel model with SBM. The observed mean vertical velocity and averaged maximum vertical velocity are shown in Fig. 1a-e. The averaged maximum vertical velocity is the mean value of the maximum vertical velocities in all penetrations for a given temperature range; each penetration has one value of maximum vertical velocity. The simulation data on the left panels include all of the ice physics implemented in the SBM, while drop-ice collision is turned off for the right panels. The modelled ice concentration is much lower than that observed by the Learjet, this may be because there are ice generation mechanisms not implemented in the model, such as ice multiplication due to large drop freezing (Lawson et al., 2015). Here we do not focus on the ice concentration but the size of ice. The Learjet measurements suggest that the ice particles observed in fresh developing convective clouds are relatively small (20-300 μm in diameter) between -7 °C and -10 °C and that the ice PSD e broadens as the temperature decreases. If drop-ice collisions are excluded, most of the modeled ice is small at warm temperatures, consistent with observation (Fig. 1h and i), only a very low concentration of large ice is found, which is from immersion

Deleted: size distributions

Deleted: ,

Deleted: liquid

Deleted: of ic

Deleted: is

Deleted: are

freezing. The deposition/condensation nucleation exhibits the largest contribution to the modelled ice (Fig. 1f-i). Immersion freezing and contact freezing contribute less to the modeled ice PSDs. If drop-ice collision is implemented, the concentration of large ice suddenly increases by 2 orders of magnitude at temperature between -7 °C and -10 °C (Fig. 1c and d), results in much broader ice PSDs than observed, indicating these large ice are from the drop-ice collision process, and are added to the ice PSDs as soon as the large drops collide with small ice assuming instantaneous freezing.

In real convective clouds, large drops do not freeze instantaneously after they are nucleated. At the early stage of freezing, large drops remain spherical or quasi-spherical (Johnson and Hallett, 1968; Murray and List, 1972; Hindmarsh et al., 2003), and probably contain more liquid mass than ice mass, so they may be regarded as liquid in the observations. Previous studies suggest it may take tens of seconds for a millimeter supercooled drop to complete freezing (Hindmarsh et al., 2003). Therefore, in strong updrafts, such as those sampled by the Learjet during ICE-T, large drops that start to freeze at warm temperatures may be fully frozen at temperatures colder than the initial nucleation temperature. However, in models, drop freezing is assumed instantaneous, so the modeled ice PSDs are much broader than observed between -7 °C and -10 °C (Fig. 1).

Examples of ice (and freezing drop) images collected by the 2D-C on the C-130 and the CPI on the Learjet are shown in Fig. 2. Both the 2D-C and CPI images were measured near the cloud top in the updraft cores of developing convective clouds. As noted in the figure, the observed particles are mostly small between -8 °C and -10 °C (Fig. 2c). Some particles may be small drops at the early stage of freezing because they exhibit slight shape deformation, as shown by the particle images in the red box in Fig. 2c; however, we have no other evidence with which to

Deleted: 3

Deleted: that

Deleted:

Deleted: and

Deleted: they are

Deleted: collided

Deleted: nucleated

Deleted: The modeled ice PSD is much broader than that observed between -7 °C and -10 °C. The deposition/condensation nucleation exhibits the largest contribution to the modeled ice PSDs (Fig. 1d). Immersion freezing, contact freezing and the Hallett-Mossop process contribute less to the modeled ice PSDs. Small ice particles are mostly formed by deposition/condensation nucleation, whereas large ice is produced by immersion freezing and drop-ice collision (Fig. 1d and h).

Deleted: are

Deleted: not

Deleted: ice

Deleted: ose

Deleted: at

Deleted: which

Deleted: ing

Deleted: ing

Deleted: l

Deleted: Previous studies have suggested that during immersion freezing, large drops have a higher probability of freezing than small drops at the same temperature (Bigg, 1953). In addition, small ice that is generated by other mechanisms (e.g., deposition/condensation nucleation, secondary ice) can be quickly collected by large drops in convective clouds, which results in the freezing of large drops. An obvious difference between the observed and modeled ice PSDs is that large ice is not observed between -7 °C and -10 °C but is found in the modeled results (Fig. 1d). There are three possible explanations for this: first, large freezing (or frozen) drops cannot be identified from the images taken by the probes, or the sampling volume of the probes is too small; second, the modeled results are not realistic; third, there could be a combination of the first and second possibilities. There is no evidence that large drops do not freeze between -7 °C and -10 °C. In the observations, only non-spherical particles are regarded as ice, but freezing drops exhibit no (obvious) shape deformation during the early stage of freezing (Johnson and Hallett, 1968; Hindmarsh et al., 2003). Due to the limitations of the instruments, freezing drops that do not exhibit obvious shape deformation cannot be identified; thus, the first possibility may apply. On the other hand, in the model simulations, drop freezing is assumed to be instantaneous, which could result in a broad ice PSD at warm temperatures; because this is not true in natural clouds, the second possibility may also apply. Therefore, the large difference between the measured and simulated ice PSDs is probably both observation- and model-related.

Deleted: particle

Deleted: ice

Deleted: comprise small frozen drops

Deleted: have just begun freezing

confirm this. Between -10 °C and -13 °C, we observe more ice particles, including both large frozen drops and small ice, as well as rimed graupel (Fig. 2a and b). Columns and plates were also observed. Considering the time that is needed for columns and plates to grow and the freezing time of large frozen drops, they were probably nucleated at a warmer temperature than is observed. Due to the relatively low resolution of the 2D-S, 2D-C, HVPS and 2D-P images, large drops at the early stage of freezing that exhibit no obvious shape deformation are regarded as drops rather than ice.

3.2 Freezing time of supercooled drops

To better interpret the freezing of large supercooled drops in strong updrafts, we analyze the freezing time and temperature of supercooled drops in this section. Fig. 3 shows the changes in drop temperature and ice mass fraction as functions of time and ambient temperature. The updraft velocity used in the calculation is the observed temperature-dependent mean vertical velocity that shown in Fig. 1a-e. Drops and air parcels ascend from -6 °C (~520 mb, ~5600 m). The nucleation temperature, which is the temperature at which drops begin to freeze, is assumed to be -8 °C. The figure demonstrates that a drop with a radius of 100 μm cools from -6 °C to -8 °C and begins to freeze at approximately 22 s. The latent heat released due to freezing leads to a sudden rise in temperature from -8 °C to 0 °C (Fig. 3a), and the ice mass fraction increases from 0 to 0.1 (Fig. 3b). It takes approximately 5 seconds for the drop to fully freeze; during freezing, the drop temperature remains at 0 °C (Fig. 3a), and the ice mass fraction continuously increases (Fig. 3b). After completely freezing, the frozen drop rapidly cools due to the large difference between the ambient temperature and the drop surface temperature. The cooling rate slows down when the frozen drop temperature approaches the ambient temperature. According

Deleted: frozen drops
Deleted: s
Deleted: generated
Deleted: freezing (or frozen)
Deleted: cannot be identified, and they
Deleted: thus
Deleted: In some spherical CPI particle images, it is also difficult to determine whether the particles have begun freezing or not, because freezing drops exhibit no (or no obvious) shape deformation during the early stages of freezing (e.g., Johnson and Hallett, 1968; Hindmarsh et al., 2003).
Deleted: understand
Deleted: impact of
Deleted: time
Deleted:
Deleted: on the modelled ice PSDs
Deleted: the observed PSDs,
Deleted: , nucleation temperature
Deleted: frozen
Deleted: with changes in
Deleted: assumed to be 10 m/s
Deleted: 23
Deleted: drop
Deleted: 4

to the equations, the cooling rate for a drop in the updraft is largely controlled by convective heat transfer, rather than radiation or diffusional growth. If significant riming occurs on the freezing (frozen) drop surface, the cooling rate could be slower, and the freezing time could thus be longer due to the latent heat release that occurs during riming (Heymsfield, 1982; Phillips et al., 2015). The drop temperature changes in a similar way for larger drops as it does for small drops. However, due to their higher terminal velocity, it takes longer for larger drops to reach their nucleation temperature (-8 °C). Drops with radii of 250 μm and 500 μm begin to freeze at 28 s and 41 s, respectively (Fig. 3a), and the ambient temperatures are approximately -8.1 °C and -8.2 °C (Fig. 3c), respectively, which is slightly colder than the drop temperature because of the gradual heat transfer from drop to air. In addition, it takes longer for larger drops to completely freeze. Drops with radii of 250 μm and 500 μm require approximately 15 s and 34 s, respectively, to fully freeze (Fig. 3a); these frozen drops are found at temperatures of -9.4 °C and -10.18 °C, respectively (Fig. 3c).

Fig. 4 shows the freezing time and frozen temperature as functions of the drop radius for different vertical air velocities and nucleation temperatures. The freezing time represents the time period from the start of drop freezing to the end of drop freezing. The figure shows that the freezing time increases as the radius increases. For the same nucleation temperature, drops freeze faster in stronger updrafts than they do in weaker ones because of the greater difference between the particle and air temperatures (Fig. 4a); however, their frozen temperatures are colder in stronger updrafts (Fig. 4b). In addition, for the same updraft strength, a drop freezes faster when its nucleation temperature is lower, and it fully freezes at colder temperatures. Moreover, for the same drop radius, the effect of the updraft strength on the freezing time is smaller if a drop nucleates at a lower temperature, as is indicated by the smaller differences between the solid,

Deleted: its

Deleted: μ

Deleted: 43

Deleted: their

Deleted: 8.15

Deleted: are

Deleted: 35

Deleted: 9.2

Deleted: 9

Deleted: 2

Deleted: .95

Deleted: the faster heat transfer rate

dashed and dotted lines for colder nucleation temperatures (Fig. 4a); however, its impact on frozen temperature does not vary substantially with different nucleation temperatures (Fig. 4b). Calculations of the freezing time and frozen temperature based on the observed temperature-dependent mean vertical velocity and the averaged maximum vertical velocity provide similar information (Fig. 4c and d). Between -7 °C and -10 °C, the observed vertical velocity is strong, so for drops larger than 400 μm in radius which start freezing at -6 °C or -8 °C, the frozen temperature is 2–3 degrees colder than the nucleation temperature. The mean vertical velocity at temperature colder than -10 °C is weaker than that between -7 °C and -10 °C, so for drops that start freezing at -10 °C, the freezing temperature is similar to the nucleation temperature (solid green line in Fig. 4d). This suggests the large frozen drops observed at -10 °C may start freezing at a temperature either warmer than or similar to -10 °C. While for the averaged maximum vertical velocity, the frozen temperature is about 1–2 degrees colder than the nucleation temperature (-10 °C) for drops with radius of 500–1000 μm.

According to Bigg (1953), large drops may begin to freeze at warmer temperatures than small drops because large drops have higher probability of containing immersion ice nuclei for a given temperature (Khain et al., 2000). Fig. 5 shows the nucleation temperature and frozen temperature as functions of the drop radius. The nucleation temperature is the temperature at which drops have a 10^{-4}% probability of freezing, as determined based on Bigg's parametrization for immersion freezing. This probability is low because of the low concentration of immersion ice nuclei that are present at warm temperatures. The figure shows that large drops may begin to freeze at warmer temperatures than small drops; however, due to their longer freezing times, large drops may fully freeze at colder temperatures than small drops if the updraft is strong enough. Immersion freezing is not the only ice nucleation mechanism. In convective clouds,

Deleted:

Deleted: t

Deleted:

Deleted: Large

Deleted: due to (Bigg, 1953).

small ice can be generated at warmer temperatures by other mechanisms (e.g., condensation/deposition nucleation). The ice PSDs measured by the Learjet indicates that ice observed between -7 °C and -10 °C are small, and larger frozen drops were observed at temperatures colder than -10 °C, but it is not known whether these large drops started to freeze before or after the small droplets, and the mechanisms that lead to drop freezing are not well understood. In models, drop freezing is assumed instantaneous, which is not realistic, would result in warmer frozen temperatures than in real clouds, as indicated by the large temperature difference between the dashed and solid lines shown in Fig. 5.

Deleted: The ice PSD measured by the Learjet indicates that large frozen drops were observed at colder temperatures than small ice

Deleted: big

3.3 Discussion

The above analysis indicates that in strong updrafts, such as that sampled by the Learjet during the ICE-T project, large drops may be fully frozen at temperatures colder than their nucleation temperature. However, if the vertical air velocity is not strong enough, large drops may descend or remain at the same level for long periods of time, and they may freeze if their temperature reaches the nucleation temperature. To illustrate this, data from a C-130 penetration is shown in Fig. 6. In this case, the penetration occurred approximately 500 m below the cloud top, as is indicated by the WCR reflectivity (Fig. 6a). The WCL power (Fig. 6c) quickly attenuated and the WCL depolarization ratio (Fig. 6d) is relatively low, which indicates that this cloud was dominated by liquid drops. At the flight level, the temperature (Fig. 6e) ranges from -4 °C to -4.5 °C in the updraft and is approximately -5 °C near the cloud edge. The maximum updraft velocity is 7 m/s, and the mean updraft velocity is approximately 3 m/s. The Doppler velocity (Fig. 6b) is negative in most areas of the clouds, indicating large particles falling through the updrafts in most areas, and its maximum value is approximately 4 m/s, indicating ascending large particles in the strongest updraft core. The 2D-C images clearly show the existence of ice

Deleted: frozen

Deleted: are

Deleted: observed

Deleted: relatively colder

Deleted: small ice in strong updrafts of convective clouds but that they may begin to freeze at warmer temperatures

Deleted: I

Deleted: a

Deleted: A

Deleted: n example of

Deleted: this

Deleted: falling

(Fig. 6f). Most of the ice particles are frozen drops and graupel, and some are needles and columns. Considering the time that is needed for the drops to freeze and for the needles and columns to grow through vapor diffusion, the observed ice (graupel, needles and columns) may have been nucleated when the cloud top was lower than observed. A previous statistical study also support that large ice present at warm temperatures in developing convective clouds with relatively weak updraft (Yang et al., 2016).

The freezing of supercooled drops may be associated with some corresponding processes. For example, drops may break up or shatter during freezing, which can produce multiple ice fragments and splinters (Lawson et al., 2015). Mason and Maybank (1960) showed that the freezing of a millimeter-sized drop may produce more than a hundred splinters. These ice splinters can enhance ice initiation in convective clouds. The Hallett-Mossop process appears to be inefficient in the strong ICE-T convective updrafts (Lawson et al., 2015), but is evidently more important in mature convective clouds with relatively weak updrafts (Heymsfield and Willis, 2014). In addition, time-dependent freezing can have an impact on the dynamics in developing clouds. The instantaneous freezing of a supercooled drop results in the sudden release of a large amount of latent heat, which may lead to an overestimation of the vertical velocity in modeled convective clouds (Fan et al., 2015). In contrast, time-dependent drop freezing can affect the cloud dynamics in a different way because its latent heat is gradually released. This study points out the need to understand drop freezing in convective clouds and allows us to interpret the deficiency of instantaneous drop freezing in cloud model up to now; however, it also raises some specific questions about ice initiation and the possible consequences of time-dependent drop freezing on cloud evolution. Answering these questions requires a better understanding of the drop freezing mechanisms in convective clouds, which in turn requires

Deleted: The graupel may fall from above; thus, they may start freezing at a colder temperature than the flight level temperature.

Deleted: is

Deleted: P

Deleted: process is

Deleted: it is

Deleted: In addition, the change in drop temperature during freezing may exert impacts on the Hallett-Mossop process. Heymsfield and Mossop (1984) showed that the Hallett-Mossop process is not only related to the ambient temperature but is also related to the graupel surface temperature. In the SBM used in this study, the Hallett-Mossop process is only parameterized for ambient temperatures between -3 °C and -8 °C. However, the Hallett-Mossop process may occur at colder ambient temperatures if the frozen drop (or graupel) surface temperature is appropriate (Heymsfield and Mossop, 1984). Fig. 3 shows that the drop temperature cools from 0 °C to its ambient temperature after being fully frozen and that the cooling rate may be even slower if there is significant riming on the surface of the particle (Phillips et al. 2015). During this process, if the drop surface temperature and other ambient conditions are suitable, the Hallett-Mossop process may occur at an air temperature that is colder than -8 °C, which could also enhance the initiation of ice in developing convective clouds. For example, a millimeter-sized frozen drop can collect approximately 600 droplets in five seconds, assuming that the droplet concentration is 50 cm^{-3} and its diameter is 20 μm. Thus, two or three ice splinters may be produced if the ambient conditions are suitable. Moreover

Deleted: Future studies are needed to explore these drop freezing-related processes.

Deleted: reveals

Deleted: importance of

Deleted: ing

Deleted: observed

Deleted: ice PSDs

Deleted: For example, it is not known why the observed "primary ice" concentration is much higher than the ice nuclei concentration (DeMott et al., 2016) and the modeled ice concentration (Fig. 1). There are several possibilities for this, including the production of ice fragments and splinters during drop freezing or the Hallett-Mossop process; droplet collisional freezing (Alkezweeny, 1969); or the electrofreezing of drops (Pruppacher, 1973). In addition, it is not known whether large drops begin freezing before or after small droplets.

Deleted: primary

more laboratory experiments to be performed and more in situ measurements to be obtained in the future.

This study focuses on relatively warm temperatures in tropical maritime developing convective clouds, with 14 penetrations between -7 °C and -10 °C, and 6 penetrations between -10 °C and -12 °C. The sample size is relatively small, but the observations are helpful for studying the ice PSDs in tropical maritime convective clouds, at least for the clouds sampled by the Learjet during the ICE-T project. Currently, there are not many measurements of PSDs in tropical maritime developing convective clouds with strong updraft cores using the-state-of-art cloud probes, especially for small ice PSDs. Clearly, more field measurements are needed in the future.

Deleted: there are

Deleted: ing

Deleted: is

Deleted: in

Deleted: and with

Deleted: , so

4. Summary

In this study, the PSDs measured in fresh developing maritime convective clouds sampled during ICE-T are shown, and the deficiency of assuming instantaneous drop freezing in models is discussed. The observations in strong convective cores presented here suggest that the observed ice is primarily small at relatively warm temperature (between -7 °C and -10 °C), but the modelled ice PSDs are much broader than observed. To interpret the difference between the modelled and the observed ice PSDs, the freezing times and temperatures of supercooled drops are calculated. This analysis indicates that the freezing time is longer for large drops than it is for small drops. In strong updrafts, such as that sampled by the Learjet during ICE-T, large freezing drops may be transported to a colder temperature than their nucleation temperature before they are fully frozen. However, in models, drop freezing is assumed instantaneous, which is not realistic, and results in much broader ice PSDs at warm temperatures. Instantaneous freezing is a reasonable assumption in models if the freezing time of supercooled drops is shorter than the

Deleted: "first ice" that is observed is small

Deleted: Due to the limitations of airborne instruments, freezing drops cannot be identified until they exhibit obvious shape deformation. If the updraft is strong enough

Deleted: brought up

Deleted: begin to exhibit obvious shape deformation

time step, but for simulations of convective clouds using models with relatively high temporal resolution, the time step may be shorter than the freezing time of supercooled drops, especially the large supercooled drops. This study aids in interpreting the modeled and observed ice PSDs in fresh developing convective clouds, drawing on the the perspective of the time required for drops to freeze. However, the mechanisms of drop freezing and ice initiation are still not well known. Future studies are required to evaluate model simulations using time-dependent drop freezing, to understand the impact of time-dependent drop freezing on the microphysics and dynamics of convective clouds, and to further explore the mechanisms of drop freezing and ice initiation.

Deleted: allows us to

Deleted: from

Deleted: freezing

Acknowledgments

This work is supported by the National Science Foundation (Awards AGS-1230203 and AGS-1034858), the National Basic Research Program of China under grant no. 2013CB955802 and the DOE Grant DE-SC0014239 as part of the ASR program. The authors acknowledge the crew of the NCAR C-130 and the SPEC Learjet for collecting these data and providing high-quality products. We thank Drs. Paul Lawson and Sarah Woods for processing and sharing the data of particle size distributions measured by Learjet.

Deleted: DE-SC0006974

Deleted: T

References

Baumgardner, D. and co-authors: Airborne instruments to measure atmospheric aerosol particles, clouds and radiation: A cook's tour of mature and emerging technology. Atmospheric Research, 102, 10-29, 2011.

Bigg, E. K.: The formation of atmospheric ice crystals by the freezing of droplets. Quarterly Journal of the Royal Meteorological Society, 79, 510-519, 1953.

Cantrell, W., and Heymsfield, A.: Production of ice in tropospheric clouds: A review. Bulletin of the American Meteorological Society, 86(6), 795-807, 2005.

DeMott, P. J. and co-authors: Sea spray aerosol as a unique source of ice nucleating particles. Proceedings of the National Academy of Sciences, 113, 5797-5803, 2016.

Dye, J. E., and Hobbs, P. V.: The influence of environmental parameters on the freezing and fragmentation of suspended water drops. Journal of the Atmospheric Sciences, 25, 82-96, 1968.

Foote, G. B., and Du Toit, P. S.: Terminal velocity of raindrops aloft. Journal of Applied Meteorology, 8, 249-253, 1969.

Hallett, J. and Mossop, S. C.: Production of secondary ice particles during the riming process. Nature, 249, 26-28, 1974.

Fan, J., Liu, Y. C., Xu, K. M., North, K., Collis, S., Dong, X., Zhang, G. J., Chen, Q., Kollias, P. and Ghan, S. J.,. Improving representation of convective transport for scale-aware parameterization: 1. Convection and cloud properties simulated with spectral bin and bulk microphysics. Journal of Geophysical Research: Atmospheres, 120, 3485-3509, 2015.

Deleted: Alkezweeny, A. J.: Freezing of supercooled water droplets due to collision. Journal of Applied Meteorology, 8, 994-995, 1969.

Heymsfield, A. J.: A comparative study of the rates of development of potential graupel and hail embryos in High Plains storms. Journal of the Atmospheric Sciences, 39, 2867-2897, 1982

Heymsfield, A., and Willis, P.: Development of first ice hydrometeors and secondary ice in a tropical oceanic deep convective cloud system near Africa. AIP Conference Proceedings, 1527, 972-975, 2013.

Heymsfield, A. J., and Willis, P.: Cloud conditions favoring secondary ice particle production in tropical maritime convection. J. Atmos. Sci., 71, 4500–4526, 2014.

Hindmarsh, J. P., Russell, A. B., and Chen, X. D.: Experimental and numerical analysis of the temperature transition of a suspended freezing water droplet. International Journal of Heat and Mass Transfer, 46, 1199-1213, 2003.

Johnson, D. A., and Hallett, J.: Freezing and shattering of supercooled water drops. Quarterly Journal of the Royal Meteorological Society, 94, 468-482, 1968.

Khain, A., Ovtchinnikov, M., Pinsky, M., Pokrovsky, A., and Krugliak, H.: Notes on the state-of-the-art numerical modeling of cloud microphysics. Atmospheric Research, 55, 159-224, 2000.

Khain, A. P. and co-authors: Representation of microphysical processes in cloud-resolving models: Spectral (bin) microphysics versus bulk parameterization. Reviews of Geophysics, 53, 247-322, 2015.

Kumjian, M. R., Ganson, S. M., and Ryzhkov, A. V.: Freezing of raindrops in deep convective updrafts: A microphysical and polarimetric model. Journal of the Atmospheric Sciences, 69, 3471-3490, 2012.

Lawson, P. R., Woods, S., and Morrison, H.: The microphysics of ice and precipitation development in tropical cumulus clouds. J. Atmos. Sci., 72, 2429-2445, 2015.

Lynn, B. H., Khain, A. P., Dudhia, J., Rosenfeld, D., Pokrovsky, A., and Seifert, A.: Spectral (bin) microphysics coupled with a mesoscale model (MM5). Part I: Model description and first results. Monthly Weather Review, 133, 44-58, 2005.

Mason, B. J. and Mayabnk, J.: The fragmentation and electrification of freezing water drops. Quarterly Journal of the Royal Meteorological Society, 86, 176-185, 1960.

Meyers, M. P., DeMott, P. J., and Cotton, W. R.: New primary ice-nucleation parameterizations in an explicit cloud model. Journal of Applied Meteorology, 31, 708-721, 1992.

Murray, W. A., and List, R.: Freezing of water drops. Journal of Glaciology, 11, 415-429, 1972.

Phillips, V. T., Khain, A., Benmoshe, N., Ilotoviz, E., and Ryzhkov, A.: Theory of time-dependent freezing. Part II: Scheme for freezing raindrops and simulations by a cloud model with spectral bin microphysics. Journal of the Atmospheric Sciences, 72, 262-286, 2015.

Pruppacher, H. R. and Klett, J. D.: Microphysics of clouds and precipitation. Atmospheric and Oceanographic Sciences Library, 954 pp, 2010.

Rangno, A. L., and Hobbs, P. V.: Microstructures and precipitation development in cumulus and small cumulonimbus clouds over the warm pool of the tropical Pacific Ocean. Quarterly Journal of the Royal Meteorological Society, 131, 639-673, 2005.

Wang, Z., Wechsler, P., Kuestner, W., French, J., Rodi, A., Glover, B., Burkhart, M., and Lukens, D.: Wyoming cloud lidar: Instrument description and applications. Opt. Express, 17,

Deleted: Pruppacher, H. R.: Electrofreezing of supercooled water. Pure and Applied Geophysics, 104, 623-634, 1973.

13576–13587, 2009.

Wang, Z. and co-authors: Single aircraft integration of remote sensing and in situ sampling for the study of cloud microphysics and dynamics. Bull. Amer. Meteor. Soc., 93, 653–668, 2012.

Yang, J., Wang, Z., Heymsfield, A. J., and Luo, T.: Liquid-Ice Mass Partition in Tropical Maritime Convective Clouds. J. Atmos. Sci., 73, 4959-4978, 2016.

Yao, S. C. and Schrock, V. E.: Heat and mass transfer from freely falling drops. Journal of Heat Transfer, 98, 120-126, 1976.

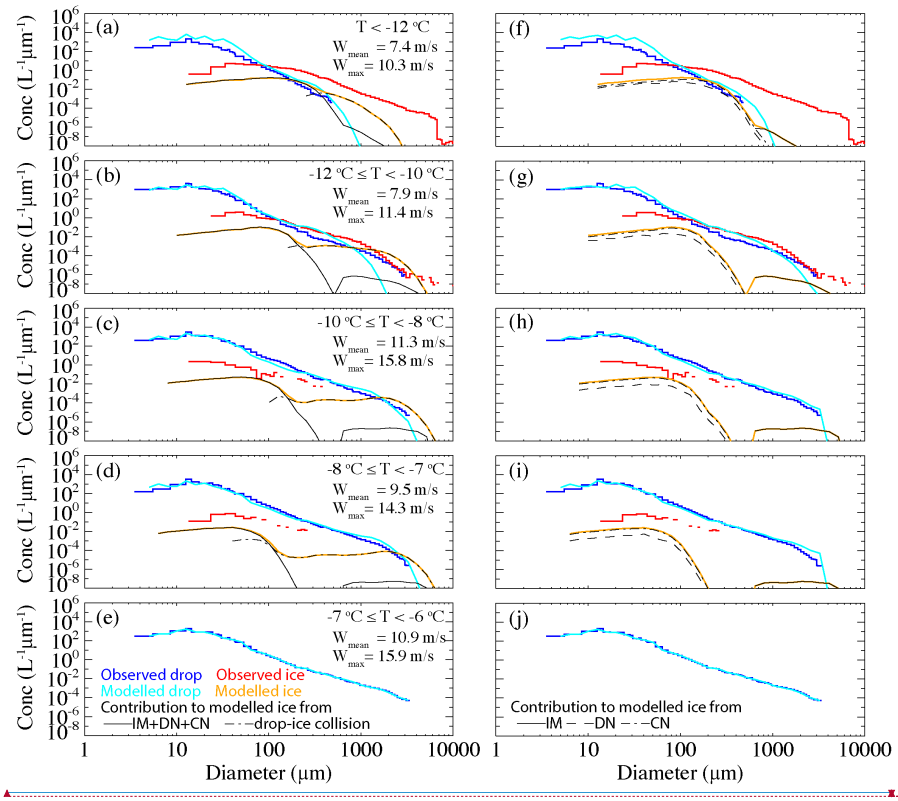

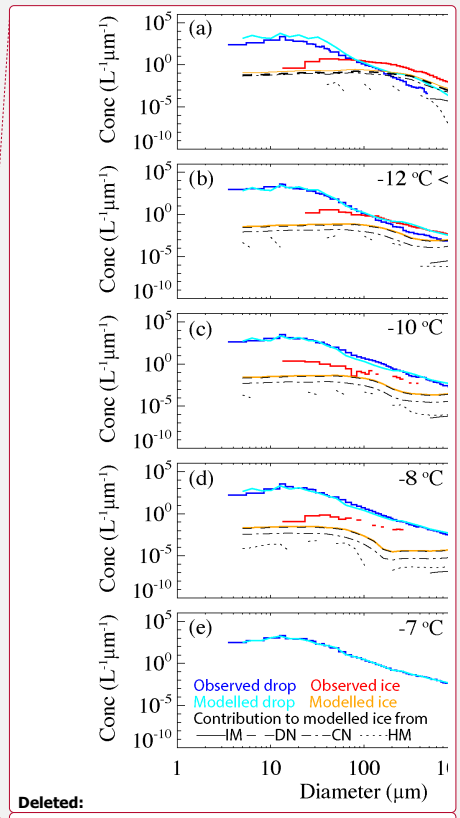

Figure 1. Particle size distributions in fresh developing convective clouds observed by the Learjet during ICE-T and those modeled using a parcel model with SBM. In (a)-(e), all of the ice physics implemented in the SBM are included; in (f)-(j), drop-ice collision is excluded. The black solid, dashed, and dashed-dotted lines in (f)-(j) represent the contributions from immersion freezing (IM), deposition/condensation nucleation (DN), and contact nucleation (CN), respectively, to the modeled ice size distributions. The black solid and dashed-dotted lines in (a)-(e) represent the contributions from primary ice nucleation (IM+DN+CN) and drop-ice collision, respectively, to the modeled ice size distributions. The observed mean vertical velocity (W_{mean}) and averaged maximum vertical velocity (W_{max}) are shown in (a)-(e).

Deleted:

Formatted: Font:(Default) Times, Font color: Text 1

Formatted: Font:(Default) Times

Formatted: Line spacing: 1.5 lines

Deleted: the left panels

Deleted: the right panels

Deleted: liquid

Deleted: , and dotted

Deleted: , and the Hallett-Mossop process (HM)

Deleted:

Formatted: Subscript

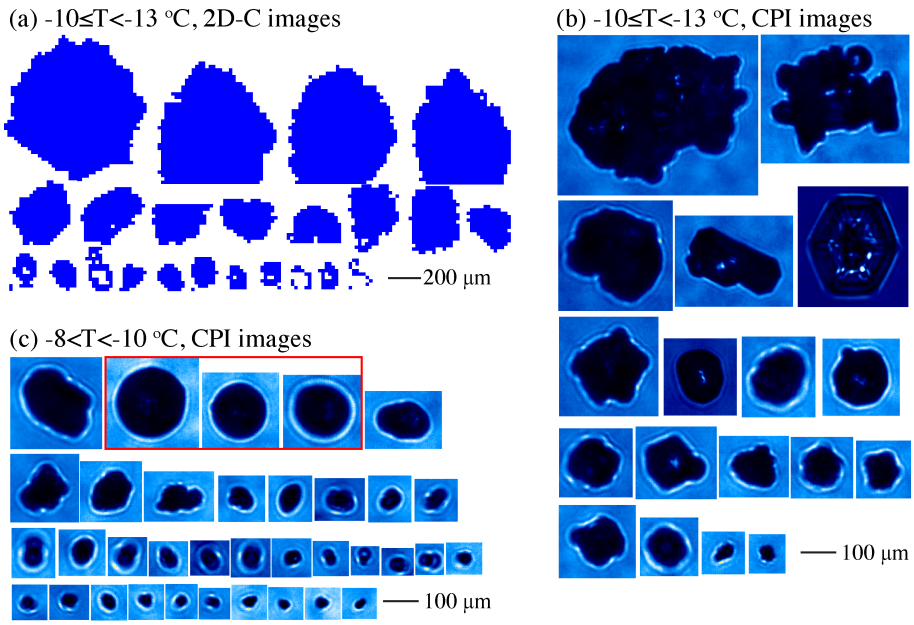

Figure 2. Examples of the 2D-C and CPI images measured in the developing convective clouds sampled during the ICE-T project.

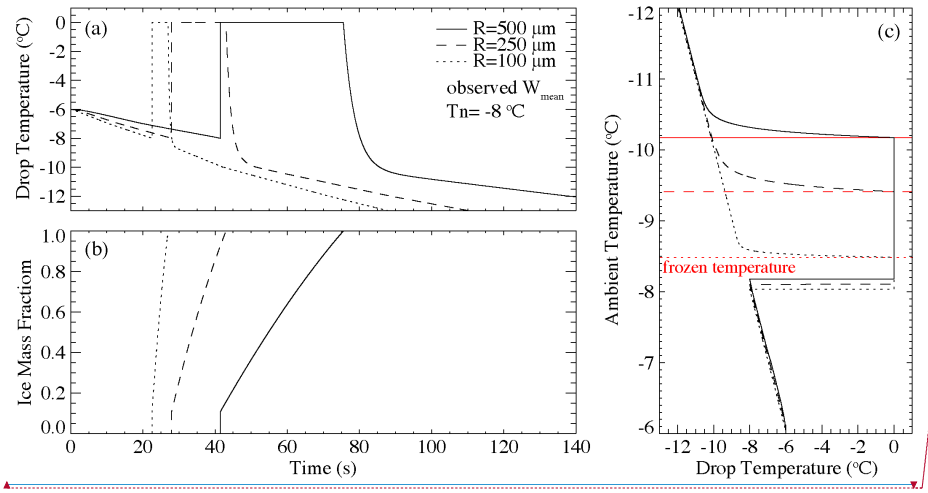

Figure 3. (a) Changes in drop temperature over time for drops with different radii based on the observed mean vertical velocity, which is temperature-dependent. Nucleation temperature (Tn) is -8 °C; (b) same as (a) but for ice mass fraction; (c) ambient temperature versus drop temperature for drops with different radii. The red solid, dashed and dotted lines indicate the frozen temperature for drops with radius of 500 μm, 250 μm and 100 μm, respectively.

Formatted: Font:(Default) Times, Font color: Text 1

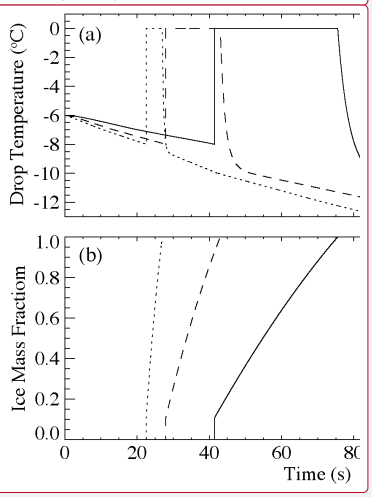

Deleted:

Deleted: Vertical air velocity (W) is assumed to be 10 m/s and n

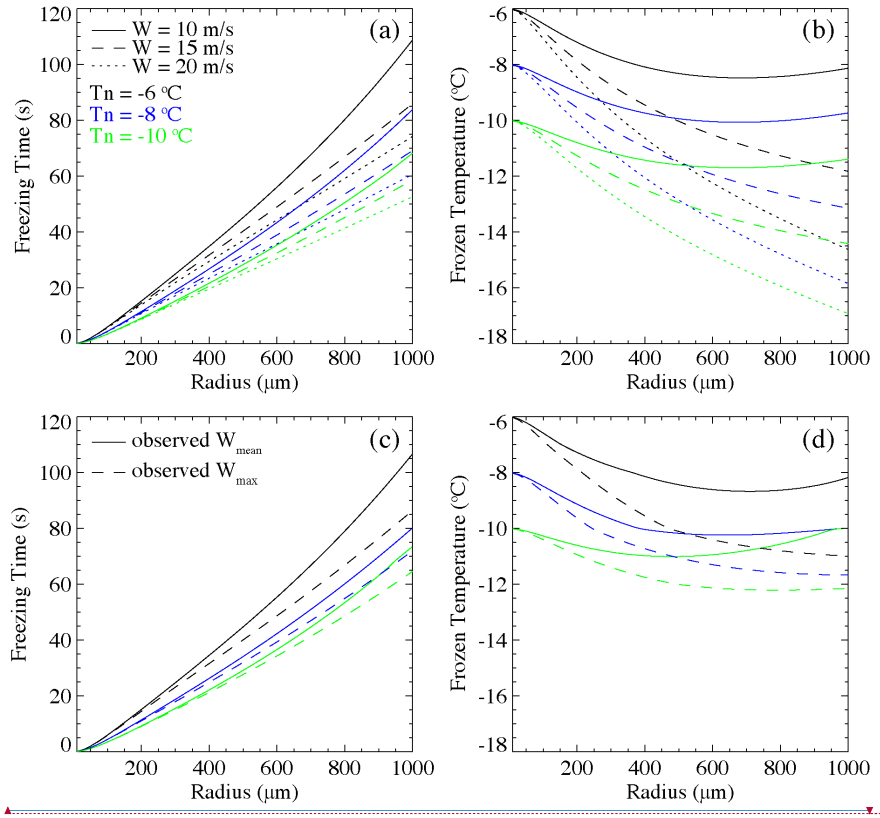

Figure 4. (a) Freezing time and (b) frozen temperature as functions of drop radius for different values of vertical air velocity (W) and nucleation temperature (Tn). (c) and (d) are the same as (a) and (b) but for the observed mean vertical velocity (W_{mean}) and averaged maximum vertical velocity (W_{max}), which are temperature-dependent.

Formatted: Font:(Default) Times, Font color: Text 1

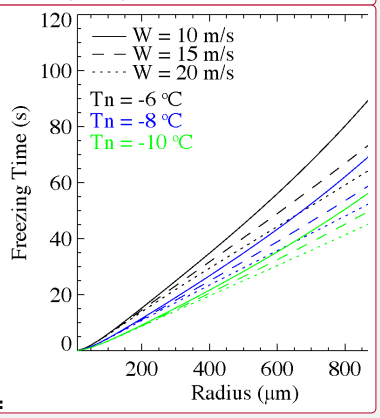

Deleted:

Formatted: Subscript

Deleted: .

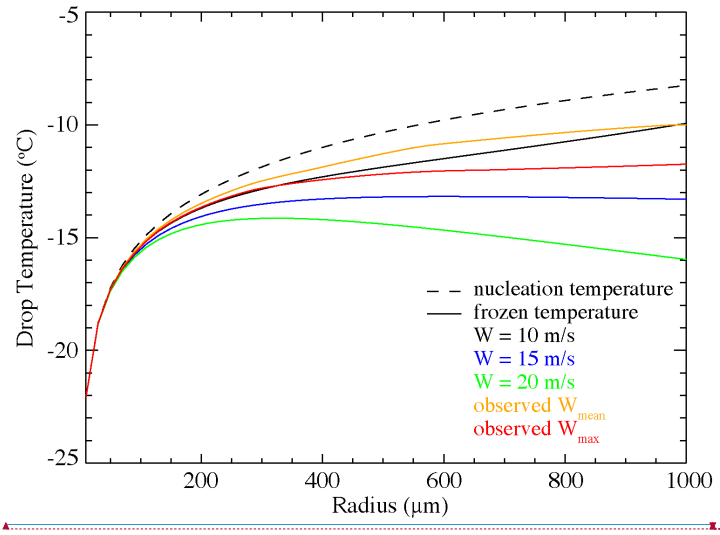

Formatted: Font:(Default) Times, Font color: Text 1

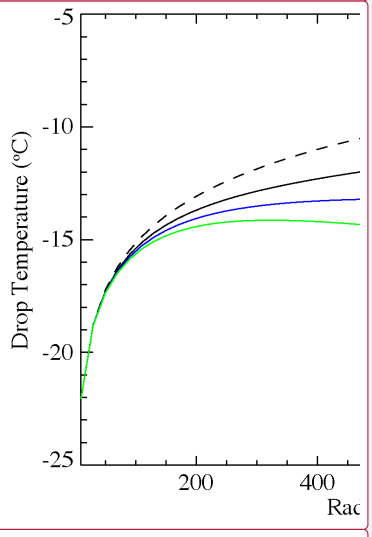

Deleted:

Formatted: Font:(Default) Times

Figure 5. Drop temperature as a function of drop radius for different vertical air velocity (W) values, including the observed mean vertical velocity (W_{mean}) and averaged maximum vertical velocity (W_{max}), which are temperature-dependent. The nucleation temperature is the temperature at which drops have a 10^{-4}% probability of freezing, as determined based on Bigg's parameterization for immersion freezing.

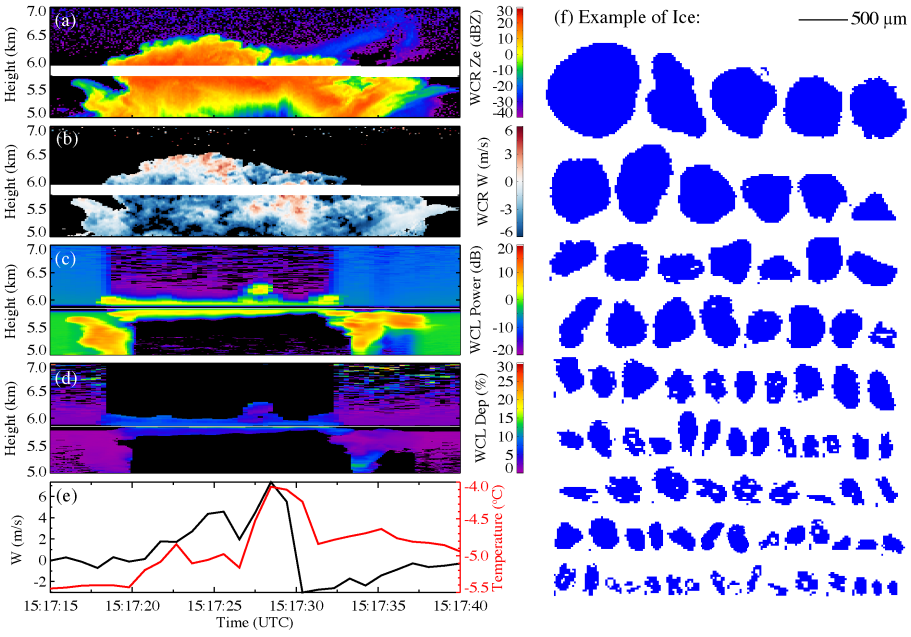

Figure 6. An example of the penetration of the C-130 in a developing cloud sampled on 23 July 2011: (a) WCR reflectivity; (b) WCR Doppler velocity; (c) WCL power; (d) WCL depolarization ratio; (e) ambient temperature and in situ vertical air velocity; and (f) examples of ice particles measured using 2D-C.